Palaeogeography, Palaeoclimatology, Palaeoecology 337–338 (2012) 14–22

Contents lists available at SciVerse ScienceDirect

Palaeogeography, Palaeoclimatology, Palaeoecology

journal homepage: www.elsevier.com/locate/palaeo

Carbon- and sulfur-isotope geochemistry of the Hirnantian (Late Ordovician) Wangjiawan (Riverside) section, South China: Global correlation and environmental event interpretation

Paul Gorjan [a,*], Kunio Kaiho [b], David A. Fike [a], Chen Xu [c]

[a] Department of Earth and Planetary Sciences, Washington University in St Louis, Campus Box 1169, 1 Brookings Drive, St Louis, Missouri 63130, USA
[b] Graduate School of Science, Tohoku University, Aoba-ku, Sendai 980-8578, Japan
[c] State Key Laboratory of Palaeontology and Stratigraphy, Nanjing, Institute of Geology and Palaeontology, Chinese Academy of Sciences, 39 East Beijing Road, 210008 Nanjing, PR China

ARTICLE INFO

Article history:
Received 24 May 2011
Received in revised form 8 March 2012
Accepted 13 March 2012
Available online 19 March 2012

Keywords:
Hirnantian
Stratigraphy
Wangjiawan
Glaciation
Carbon isotopes
Sulfur isotopes

ABSTRACT

Detailed geochemical analyses ($\delta^{13}C_{carb}$, $\delta^{13}C_{org}$, $\delta^{34}S_{sulfide}$, and abundance of sulfide, carbonate and organic carbon) were performed on samples from the Wangjiawan (Riverside) section, close to the GSSP (Global Stratotype Section and Point) for the Hirnantian stage of the Ordovician. New data show two increases in carbonate content coincident with two glacial pulses that reduced detrital input. The new $\delta^{34}S_{sulfide}$ data show distinct changes in this section, with relatively high values in the Kuanyinchiao Formation, a pattern observed throughout the Yangtze Platform. However, there is no consensus on the cause of these changes. The new $\delta^{13}C_{carb}$ data show a sharp rise and peak in the *extraordinarius* zone, below the previously published $\delta^{13}C_{org}$ peak in the *persculptus* zone. A compilation of the new results with other sections indicates the Hirnantian carbon-isotope excursion starts near the *pacificus–extraordinarius* boundary and elevated values remain until the end of the excursion in the *persculptus* zone for both $\delta^{13}C_{org}$ and $\delta^{13}C_{carb}$. The controversy over correlating Hirnantian graptolite zones with chitinozoan zones can also be addressed. The new $\delta^{13}C_{carb}$ data also allow direct comparison with Hirnantian $\delta^{13}C_{carb}$ data from Anticosti Island and the Baltic region, which are zoned by chitinozoan fossils. This comparison favors a correlation of the *taugourdeaui* and *scabra* chitinozoan zones with the *extraordinarius* graptolite zone.

1. Introduction

The Hirnantian stage of the Late Ordovician hosts a confluence of several significant events, including a glaciation, sea level changes, a severe mass extinction, and a global positive carbon-isotope ($\delta^{13}C$) excursion (e.g., Finney et al., 1999; Melchin and Holmden, 2006; Fan et al., 2009; LaPorte et al., 2009; Young et al., 2010; Jones et al., 2011). The relationship between these events is only partially understood and the initial cause of the glaciation and its relationship to the carbon cycle perturbation remain unknown.

The Hirnantian glaciation was recognized from glacial sediments in north Gondwana (Saharan Africa, South Africa and Arabia) (Deynoux and Trompette, 1981; Deynoux, 1985; Ghienne, 2003; Ghienne et al., 2007; Le Heron et al., 2007). Trotter et al. (2008) used temperature-dependent oxygen isotopes ($\delta^{18}O_{apatite}$) in Ordovician conodonts to show a global temperature fall in the late Ordovician. This conclusion was reinforced by clumped-isotope paleothermometry on Hirnantian calcites (Finnegan et al., 2011) that shows cooling and rapid ice accumulation at this time — perhaps twice the ice volume as the Last Glacial Maximum. Detailed geochemical and sedimentological work has identified more than one episode of glacial advance and retreat (Ghienne, 2003; Yan et al., 2010).

The Hirnantian extinction is recognized as the second most devastating extinction in the Phanerozoic, after the Permian–Triassic extinction, with the elimination of about 86% of species (Sheehan, 2001; Bambach et al., 2004). Although a gradual decline in biodiversity is recognized during the Katian (Kaljo et al., 2011), fine-scaled paleontological work demonstrates that the greatest loss was across the Katian–Hirnantian boundary (Brenchley et al., 1994; Sheehan, 2001; Rong et al., 2002; Chen et al., 2005a; Fan et al., 2009), thought to coincide with the onset of a severe cooling (Finnegan et al., 2011). This coincidence has provided a solid case for linking the extinction with decreased temperature and a drop in sea level, the latter, in turn, eliminating vast epeiric sea habitats (Brenchley et al., 1994; Sheehan, 2001). Further graptolite and brachiopod extinctions also occur later in the Hirnantian (Rong et al., 2002; Chen et al., 2005a; Fan et al., 2009).

The Hirnantian stage also records a sharp perturbation in the carbon cycle, seen in the enrichment of ^{13}C in both sedimentary carbonate and organic matter. Some have attributed this to an increased burial of organic matter (e.g., Brenchley et al., 2003). An alternative hypothesis

* Corresponding author. Tel.: +1 314 935 9088.
E-mail address: pgorjan@levee.wustl.edu (P. Gorjan).

0031-0182/$ – see front matter © 2012 Elsevier B.V. All rights reserved.
doi:10.1016/j.palaeo.2012.03.021

is that a global regression exposed carbonate platforms that were then preferentially weathered, resulting in an increase in riverine $\delta^{13}C$ (Kump et al., 1999; Melchin and Holmden, 2006). This would then drive a corresponding increase in oceanic $\delta^{13}C$ composition.

The uncertainty in correlating sections from different continents has hampered the study of the glaciation, the mass extinction, and the changes in carbon cycling that mark the Hirnantian (Delabroye and Vecoli, 2010). There is no one correlative fossil group (graptolites, chitinozoans, brachipods or conodonts) present in all sections worldwide. Graptolites are common in the shaly deposits of South China, where the GSSP at Wangjiawan (North) is established, but the carbonate-dominated successions of Anticosti Island and Estonia are dominated by conodont and chitinozoan fossils (Soufiane and Achab, 2000; Copper, 2001; Brenchley et al., 2003; Kaljo et al., 2008; Achab et al., 2011); graptolites from these areas are only tenuously related to Chinese graptolites (Riva, 1988; Melchin, 2008; Young et al., 2010). It is similarly challenging to correlate Gondwanan glacial sediments with tropical sections that often have the best fossil and isotope records. Thus, precisely comparing the timing of the glacial onset with other (biological and geochemical) events is difficult.

Furthermore, the use of carbon isotopes to correlate sections has not been straightforward (Chen et al., 2006; Delabroye and Vecoli, 2010). To date no Chinese section – including the GSSP section for the Hirnantian stage (Wangjiawan North) – has any published carbonate-carbon isotope ($\delta^{13}C_{carb}$) data, which is the most commonly used chemostratigraphic tool (e.g., Gradstein et al., 2004).

This study presents high-resolution (cm-scale) characterization of carbon- and sulfur-cycling, including isotopic ($\delta^{13}C_{carb}$, $\delta^{13}C_{org}$, $\delta^{34}S_{sulfide}$) and abundance (sulfide, or %S, and total organic carbon, or TOC) data, across the Hirnantian interval of the Wangjiawan (Riverside) section in order to constrain changes in the local geochemistry as well as linking these to global trends in $\delta^{13}C_{carb}$, organic deposition (TOC), and the glaciation.

2. Geology, stratigraphy and the extinction boundary

Numerous studies have been published on the Late Ordovician of the Yangtze platform, including biostratigraphic (e.g., Chen et al., 2000; Vandenbroucke et al., 2005), paleogeographic (Zhang et al., 2000; Chen et al., 2004), chemostratigraphic (Chen et al., 2005b; Fan et al., 2009), as well as carbon and sulfur isotope-event studies (Yan et al., 2008, 2009; Zhang et al., 2009).

The Wangjiawan site was an outer shelf location on the South China craton during the Ordovician–Silurian transition (Chen et al., 2004; Fig. 1A). The Wufeng, Kuanyinchiao and Lungamachi Formations span the uppermost Ordovician and Lower Silurian, in ascending order. The Wufeng and Lungamachi Formations are comprised of dark shales and occasional chert with abundant graptolite fossils (Chen et al., 2000; Chen et al., 2006). The Kuanyinchiao Formation is a thin (less than 50-cm thick) argillaceous limestone that contains abundant shelly fossils (Hirnantian fauna) (Chen et al., 2000). The Kuanyinchiao Formation marks a drop in eustatic sea level (Fan et al., 2009) and the associated Hirnantian fauna are recognized as cool/cold water fauna (Rong et al., 2002). This is consistent with global cooling and sequestration of water into Gondwanan ice caps during the Hirnantian glacial episode.

The Wangjiawan (Riverside) section is found on the banks of the Wangjiawan River by the southeastern end of Wangjiawan village, located about 42 km north of Yichang city. The Wangjiawan (North) section, located ~180 m northwest of the Riverside section, hosts the Global Stratotype Section and Point (GSSP) for the Hirnantian (Late Ordovician) (Fig. 1B). The Riverside section is less weathered than the North section and thus provides better material for geochemical analysis.

3. Methods

An almost continuous section of approximately 2.5 m of sedimentary rock was sampled across the Hirnantian interval at the Wangjiawan (Riverside) section (Fig. 1B). Samples were chipped and pieces without weathering or veining were selected for powdering.

Sedimentary sulfide was extracted from 0.1 to 0.3 g of powdered sample for $\delta^{34}S_{sulfide}$ analysis. The sulfide extraction procedure is based on the method presented by Burton et al. (2008). The sample was placed in a tube along with an inner vial of zinc acetate solution. The tube was sealed with a cap and the air removed under vacuum. Acidified 6 M chromium(II) chloride solution was then injected into the tube through an opening. The mixture was shaken for 48 h. The Cr(II) ions reacted with any sulfide to form H_2S, which then diffused to the zinc acetate solution to form solid ZnS. The ZnS was then centrifuged, rinsed and dried. The sulfide content (%S) was determined by boiling some powdered sample in acidified Cr(II) solution and collection of the evolved H_2S as Ag_2S in a silver nitrate solution. The dried Ag_2S was then weighed and the %S calculated (Canfield et al., 1986).

Total organic carbon (TOC) was determined by treating powdered samples with 6 M HCl to remove carbonate. The sample was then rinsed to remove the acid. The mass difference between the original sample and acid-treated residue was used to determine carbonate content. The dried sample was then combusted and the evolved CO_2 analyzed on the mass spectrometer. During the mass spectrometric analysis the sample peak height was calibrated against organic carbon standards to estimate the organic carbon content.

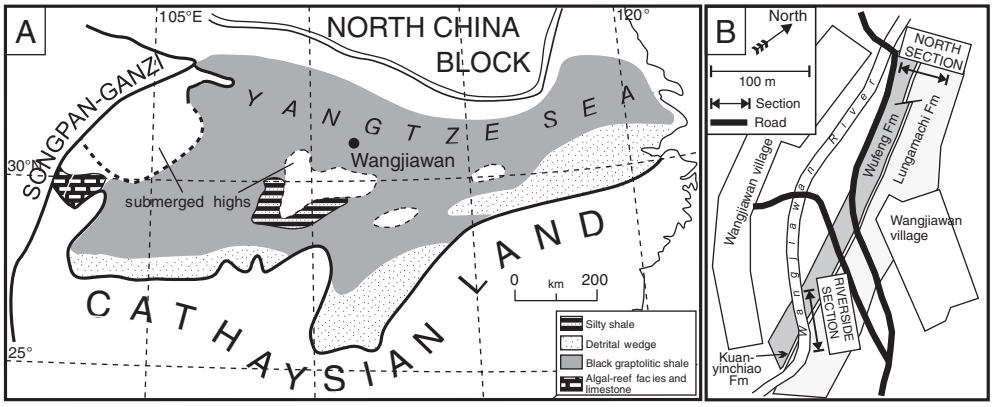

Fig. 1. (A) Paleogeographical map of the Hirnantian Yangtze Platform showing location of the Wangjiawan site and extent of the epeiric Yangtze Sea at Wufeng Formation time. (B) Map showing location of Wangjiawan (Riverside) and Wangjiawan (North) sections adjacent to the Wangjiawan village, Hubei, China. The Kuanyinchiao Formation is exposed between the Wufeng and Lungamachi Formations, and its thickness exaggerated to make it easily seen. Sampling was performed about a meter on either side of the Kuanyinchiao Formation. (A) is after Chen et al., 2004, (B) is adapted from Chen et al., 2006.

Isotopic determinations for sulfide ($\delta^{34}S_{sulfide}$) were carried out using a Costech ECS 4010 Elemental Analyzer coupled to a Thermo-Finnigan Delta V Plus mass spectrometer. Approximately 300 μg of ZnS was combusted in a tin cup at 1000 °C, and the evolved SO_2 gas is then sampled by the mass spectrometer. Sulfur-isotope compositions ($\delta^{34}S$) were calibrated against NBS-127, IAEA-S1, and IAEA-S3 and are expressed as a permil (‰) deviation, relative to the V-CDT (Vienna Canyon Diablo Troilite) scale. Reproducibility, based on replicate analyses is better than 0.4‰ (1σ).

Isotopic determinations for organic carbon ($\delta^{13}C_{org}$) were carried out using the above elemental analyzer–mass spectrometer system. Approximately 300 μg of acidified sample was combusted at 1000 °C, and the evolved CO_2 gas was then sampled by the elemental analyzer–mass spectrometer. Carbon-isotope compositions were calibrated against IAEA-NBS-21 graphite, IAEA-C6 sucrose and in-house acetanilide standards and are expressed as a permil (‰) deviation, relative to the V-PDB (Vienna Pee Dee Belemnite) scale. Duplicate samples were reproducible within 0.25‰ (1σ).

Carbonate carbon isotopes ($\delta^{13}C_{carb}$) were carried out using a Thermo-Finnigan Gas Bench II coupled to a Delta V Plus mass spectrometer. Approximately 150 μg of bulk-powdered sample was reacted for 4 h at 72 °C with excess 100% phosphoric acid in a helium-flushed, sealed tube. The evolved CO_2 was then sampled by the gas bench–mass spectrometer. Isotopic measurements were calibrated against NBS-19, NBS-20, and two in-house standards, with analytical errors of 0.2‰ (1σ) for $\delta^{13}C_{carb}$ and 0.4‰ (1σ) for $\delta^{18}O_{carb}$ and are expressed as a permil (‰) deviation relative to the V-PDB (Vienna Pee Dee Belemnite) scale.

4. Results

The $\delta^{13}C_{carb}$ profile shows a positive excursion from about −4‰ to −1‰, beginning in the *extraordinarius* zone, with a sharp negative spike down to −8‰ in the Kuanyinchiao Formation. A return to pre-excursion values occurs in the *persculptus* zone of the Lungamachi Formation. Carbonate content is less than 5% for the *pacificus* zone except in the uppermost 2 cm where it begins to rise, peaking at ~60% in the basal *extraordinarius* zone. Carbonate then declines to 10–30% until a second peak at ~85% in the Kuanyinchiao Formation (Hirnantian Fauna zone). Values drop abruptly to under 10% at the start of the Lungamachi Formation.

The $\delta^{13}C_{org}$ generated in this study is broadly consistent with previously published $\delta^{13}C_{org}$ data for the Wangjiawan (Riverside) section (Chen et al., 2005b; Fan et al., 2009). However, the new data show a higher peak and steeper decline in the upper Kuanyinchiao Formation (Hirnantian Fauna zone), probably due to the greater sampling density of this study. This sharp decline in $\delta^{13}C_{org}$ within the Hirnantian Fauna zone is also seen at the Wangjiawan (North) (Wang et al., 1997; Fan et al., 2009), Huanghuachang (Wang et al., 1997), Nanbazi (Yan et al., 2009), and Fenxiang (Wang et al., 1997) sections within China. In the Lungamachi Formation some $\delta^{13}C_{org}$ values vary by 1 to 1.5‰ from previously published values (Fig. 2). The reason for this is uncertain.

Total organic carbon (TOC) is generally above 5% in the Wufeng Formation, but dips sharply in the Kuanyinchiao Formation and remains low (<1%) until the Lungamachi Formation. Peak $\delta^{13}C_{org}$ values occur in the low TOC interval. However, $\delta^{13}C_{org}$ appears to move independently of TOC. Even the transitions from low to high (or high to low) TOC in the Wufeng and Lungamachi Formations (2–10%) do not affect the $\delta^{13}C_{org}$ signals.

The new $\delta^{34}S_{sulfide}$ results produced a smooth profile between −20‰ and −10‰ in the *pacificus* and lower *extraordinarius* zones. The upper *extraordinarius* zone exhibits a large range of values, but then the smooth profile resumes in the Kuanyinchiao Formation (Hirnantian Fauna zone), although values are about 20‰ heavier than in the *pacificus* zone. In the overlying Lungamachi Formation values return to the pre-excursion baseline of around −20‰. These $\delta^{34}S_{sulfide}$ profiles are consistent with previously published results from the Wangjiawan (North), Nanbazi (Yan et al., 2009) and Honghuayuan (Zhang et al., 2009) sections, all of which document an ~20‰ enrichment in $\delta^{34}S_{sulfide}$. Further upsection into the Silurian (*ascensus* zone and above) $\delta^{34}S_{sulfide}$ values are highly variable, between −30‰ and +22‰.

5. Discussion

5.1. Sulfur geochemistry

Sulfide in the sediment comes mainly in the form of pyrite. It is produced by sulfate reducing bacteria, which metabolize sulfate (SO_4^{2-}) to sulfide (S^{2-}). The sulfide then reacts with any available iron in the sediment to form pyrite (FeS_2), a stable mineral that is preserved in sediments (Goldhaber and Kaplan, 1974). The metabolic activity of the sulfate reducing bacteria generally depletes (or fractionates) the resulting sulfide in ^{34}S, by up to 70‰ (Goldhaber and Kaplan, 1974; Canfield, 2001; Sim et al., 2011a). The final isotopic composition of sulfide is determined by the isotopic composition of the source sulfate, and the magnitude of fractionation, which depends on various factors. Firstly, metabolic activity generally results in minimal fractionation under sulfate-limited conditions where most of the sulfate will be metabolized. Secondly, increasing the rate of bacterial sulfate reduction, by increasing the amount and reactivity of organic matter (Berner, 1984), will reduce the amount of fractionation (Habicht and Canfield, 1997; Canfield, 2001; Habicht and Canfield, 2001; Sim et al., 2011b). Thirdly, increasing the presence of additional sulfur cycles (i.e., partial sulfide oxidation to elemental sulfur (S^0) followed by disproportionation, forming sulfide and sulfate from S^0), will increase the fractionation (Habicht and Canfield, 1997; Canfield, 2001; Habicht and Canfield, 2001). Sedimentation rate has also been cited in affecting $\delta^{34}S_{sulfide}$ (Goldhaber and Kaplan, 1974), although this is probably because of the way it affects the supply of organic matter (Berner, 1978) and sulfate (Chambers, 1982).

The new $\delta^{34}S_{sulfide}$ data show values from −20‰ and −14‰ in the *pacificus* zone but form a very tight cluster around −10‰ across the *pacificus–extraordinarius* boundary and through much of the *extraordinarius* zone, despite other major geochemical changes at this time, including sharp changes in sulfide content. The fact that $\delta^{34}S_{sulfide}$ is little changed would indicate that those factors most responsible for the fractionation of sulfur isotopes (i.e., the sulfate $\delta^{34}S$ and availability, reduction rate, and disproportionation) were surprisingly stable. Yan et al. (2008) suggested this boundary hosted a change from euxinic to oxic conditions from iron, carbon and sulfur studies from the Wangjiawan (North) section. However, the constant $\delta^{34}S_{sulfide}$ values suggest this did not occur, as a change in sulfide source would generally bring a change in $\delta^{34}S_{sulfide}$. Alternatively, the redox change may have occurred 10–20 cm below the *pacificus–extraordinarius* boundary, where the $\delta^{34}S_{sulfide}$ pattern changes slightly.

In the upper *extraordinarius* zone, just before the Kuanyinchiao Formation, $\delta^{34}S_{sulfide}$ fluctuates between about −20‰ and +15‰. There is little change in TOC or carbonate deposition and redox indicators from the Wangjiawan (North) section (reactive iron and degree of pyritization; Fig. 2) suggest the water column was still oxygenated (Yan et al., 2008). Yan et al. (2010) determined a chemical alteration index (CAI) – a compilation of cation ratios that indicate weathering rates – that shows a coincident shift to greater weathering, i.e., a less arid interglacial episode (Fig. 2). However, the cause of the $\delta^{34}S_{sulfide}$ variability is uncertain. It could be due to changes in sulfate $\delta^{34}S$, sulfate availability or disproportionation as the relevant factors. Although distinguishing between these requires other data.

In the Kuanyinchiao Formation there is a $\delta^{34}S_{sulfide}$ increase, with values consistently elevated, from about −6‰ to +4‰. TOC values plunge below 1%. Two hypotheses have been proposed to explain this $\delta^{34}S_{sulfide}$ excursion. Yan et al. (2009) interpret the heavier $\delta^{34}S_{sulfide}$

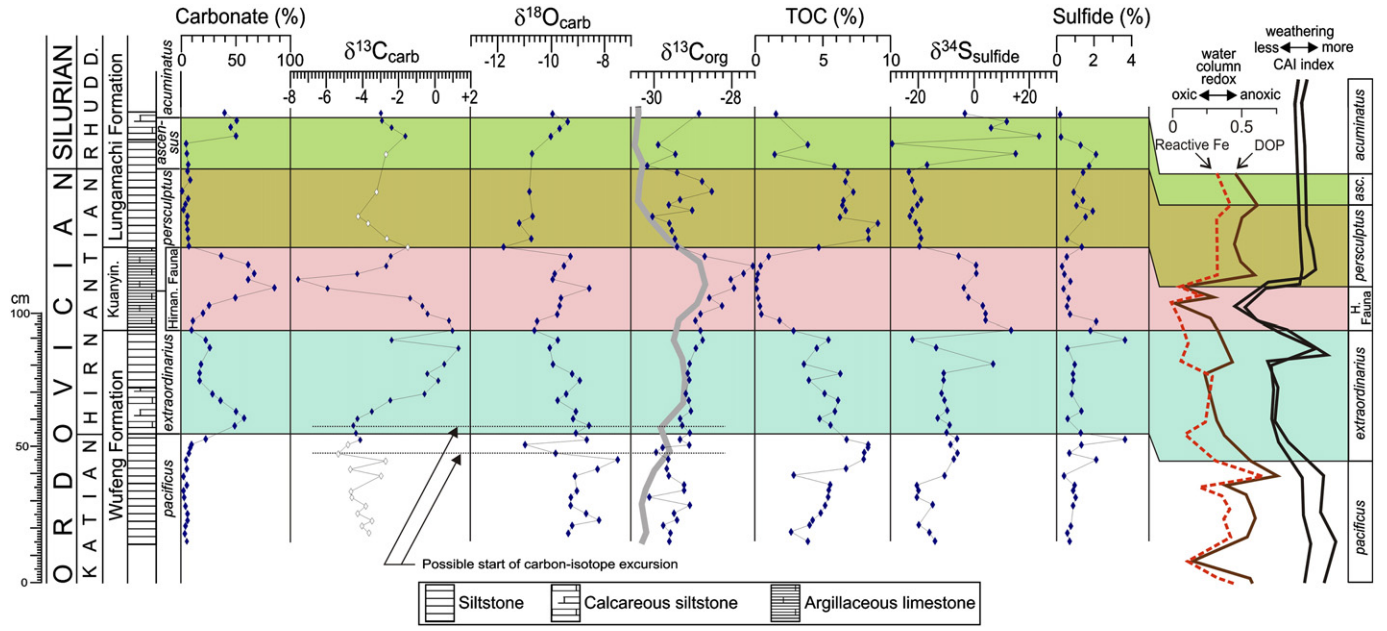

Fig. 2. New geochemical data covering the Hirnantian portion of the Wangjiawan (Riverside) section, South China. White $\delta^{13}C_{carb}$ data points may be influenced by organic matter oxidation (discussed in Section 5.2). Water column redox and weathering data from the Wangjiawan (North) section. Start of the carbon isotope excursion, taking into account both carbonate and organic carbon, is judged as the inflection point where values begin to form the ascending limb of the excursion.
Formations and graptolite zonation from Chen et al. (2006). Published $\delta^{13}C_{org}$ data (gray line) from Chen et al. (2006) and Fan et al. (2009). CAI (chemical alteration index) and associated Wangjiawan (North) graptolite boundaries from Yan et al. (2010). Reactive iron (dashed red line) and degree of pyritization (DOP; solid black line) from Yan et al. (2008). Kuanyin. = Kuanyinchiao; Hirnan. = Hirnantian; Rhudd. = Rhuddanian.

values as a change from anoxic to oxic waters that forced the sulfate reducing bacteria further into the sediment, where sulfate can become limited because the supply of water, and therefore sulfate, from the overlying water column is limited. However, Zhang et al. (2009) suggest that the increase in $\delta^{34}S_{sulfide}$ was caused by a proportional increase in seawater sulfate $\delta^{34}S$ on the Yangtze Platform, the sulfate $\delta^{34}S$ rise being caused by the rapid burial of sulfide, and organic carbon, in local anoxic deep-water sub-basins, although such a situation has not yet been demonstrated in modern or ancient settings. It is also possible that bacterial reduction rate increased through the delivery of a more reactive type of organic matter, albeit less of it. Alternatively, it is possible that the new environment of the Kuanyinchiao Formation had hosted a different mix of sulfur cycling bacteria that may not have disproportionated sulfur as much.

The Kuanyinchiao–Lungamachi boundary hosts a sharp transition to anoxic or euxinic conditions (Yan et al., 2008) with high TOC and high sulfide contents, associated with the deglaciation (Fig. 2). $\delta^{34}S_{sulfide}$ is consistently around −20‰ in the *persculptus* zone. These values are at least 10‰ lower than the sulfides of the lower *extraordinarius* zone. This can be explained as the result of anoxic conditions allowing bacterial sulfate reduction to occur at or above the sediment–water interface, thereby having an unlimited sulfate supply, i.e., the hypothesis of Yan et al. (2009). However, this explanation is not consistent with the $\delta^{34}S_{sulfide}$ values in the overlying *ascensus* zone, which are erratic, fluctuating from −30‰ to +22‰, even though there is no apparent change in redox conditions (Fig. 2). Again, the reactivity of the organic matter or changing bacterial populations may be the cause of this, but further work is required to test this.

The new $\delta^{34}S_{sulfide}$ data from the Wangjiawan (Riverside) section (Fig. 2) are broadly consistent with results at other Yangtze Platform sections: the Wangjiawan (North) and Nanbazi sections (Yan et al., 2009), as well as the Honghuayuan section (Zhang et al., 2009). All data sets show a rise in $\delta^{34}S_{sulfide}$ in the upper Wufeng Formation and an abrupt drop at the Kuanyinchiao–Lungamachi transition. The consistency in $\delta^{34}S_{sulfide}$ patterns over such widespread sections (hundreds of kilometers apart) indicates that the mechanism operates basin-wide.

In short, there is no simple and consistent explanation for the $\delta^{34}S_{sulfide}$ values in this section. Increased TOC can increase bacterial reduction rate, which in turn increases the $\delta^{34}S_{sulfide}$. But TOC has no apparent effect in this section (in fact the intervals with lowest TOC have the highest $\delta^{34}S_{sulfide}$). Likewise, changing sedimentation conditions, as recorded by carbonate content, also has no effect.Availability of sulfate is consistent with controlling $\delta^{34}S_{sulfide}$ in some portions of this section, but not all. Changing sulfate $\delta^{34}S$ is also a possibility but further work, perhaps on carbonate-associated sulfate, is required to test this. Changing of organic matter reactivity, thereby encouraging or discouraging higher bacterial metabolic rates, could be the cause but organic geochemical work is required to investigate this. Alternatively, changes in the bacterial communities may be a solution but this cannot be tested in ancient strata.

5.2. Reliability of $\delta^{13}C_{carb}$ as a primary signal

The new $\delta^{13}C_{carb}$ results show a positive excursion in the *extraordinarius* zone. This excursion matches the timing and magnitude of other known Hirnantian $\delta^{13}C_{carb}$ excursions from sections around the world where graptolite biostratigraphic analysis has been done (Fig. 3). This is strong evidence that this signal is derived from Hirnantian seawater. However, the absolute values are shifted to the negative by about 3–4‰ compared to the $\delta^{13}C_{carb}$ of most other sections where the baseline is about 0‰ (Fig. 3).

Differences in $\delta^{13}C_{carb}$ values between open ocean and platform settings, and even different parts of platforms, have been demonstrated in modern and ancient settings (Patterson and Walter, 1994; Immenhauser et al., 2002, 2003; Panchuk et al., 2005, 2006; LaPorte et al., 2009; Cramer et al., 2010). The more proximal platform sites can have either more negative or more positive $\delta^{13}C_{carb}$ values. In some modern settings $\delta^{13}C_{carb}$ is more negative compared to the open ocean due to ^{13}C-depleted organic matter being oxidized but not adequately mixed with the open ocean (Patterson and Walter, 1994), commonly referred to as 'aging' of waters. However,

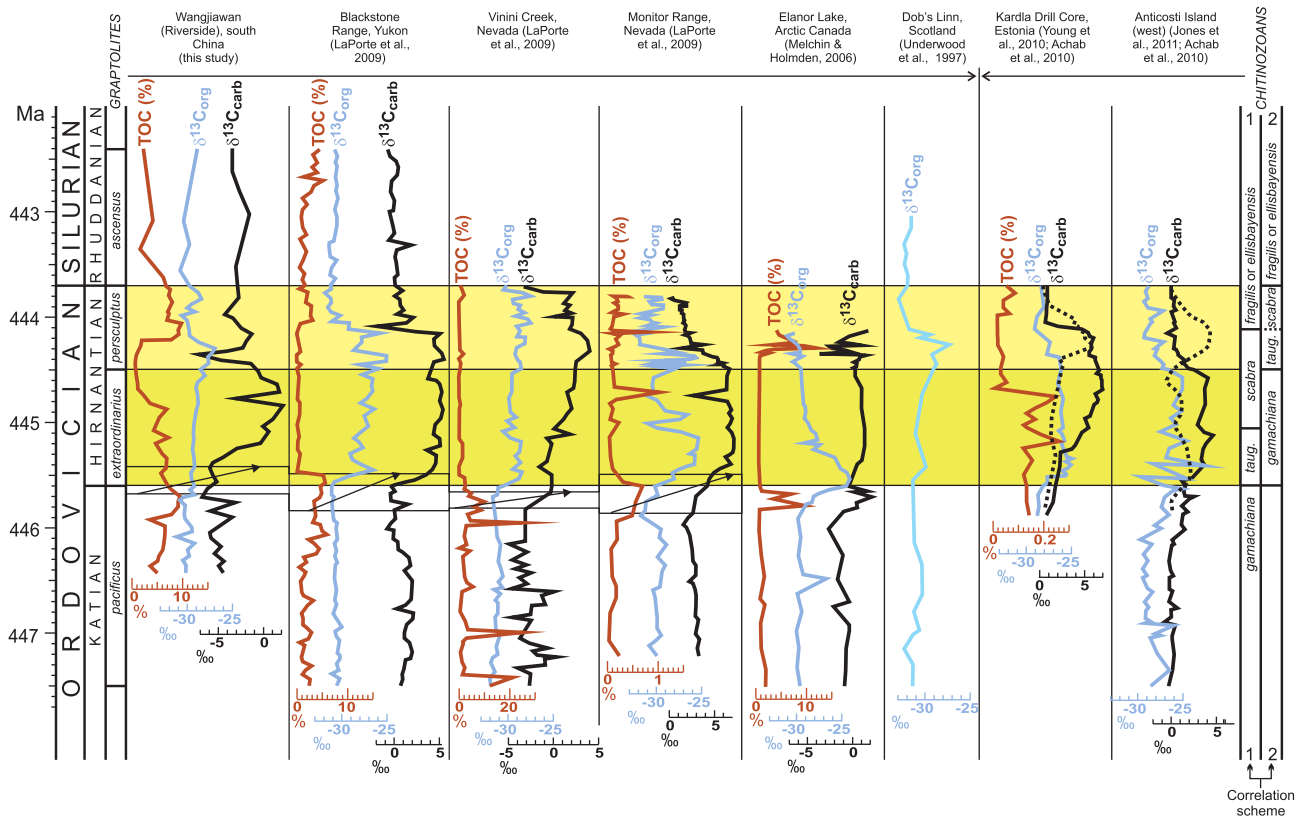

Fig. 3. TOC (weight %), $\delta^{13}C_{org}$ (‰), $\delta^{13}C_{carb}$ (‰) profiles across the Ordovician–Silurian transition. All sections correlated by graptolite biozones except the Kardla Drill Core (Estonia) and Anticosti Island (Canada), which are correlated using chitinozoan biozones. Kardla Drill Core and Anticosti Island are correlated to the other sections assuming *taugourdeaui* and *scabra* zones sit at the base of the Hirnantian (scheme 1), as justified in Section 5.3. Dashed $\delta^{13}C_{carb}$ profiles are rescaled according to Achab et al. (2011) showing what the $\delta^{13}C_{carb}$ would look like if plotted according to the scheme *taugourdeaui* + *scabra* = *persculptus* (scheme 2). Note variation in TOC scale, but $\delta^{13}C_{org}$ and $\delta^{13}C_{carb}$ scales are consistent between sections. The diagonal arrows indicate stratigraphic intervals of rapid sedimentary carbonate accumulation. Geochemical data is fixed at the zone boundaries and linearly interpolated between the zone boundaries for sections other than the Wangjiawan (Riverside). The Dob's Linn curve, originally from Underwood et al. (1997) is redrawn according to biozones by Melchin et al., 2003. Timescale according to Ogg et al. (2008). *taug.* = *taugourdeaui*.

cases from the Silurian (Cramer et al., 2010) and Ordovician (LaPorte et al., 2009) show the more proximal sediments having more positive $\delta^{13}C_{carb}$ values. The causes for these $\delta^{13}C_{carb}$ offsets are still debated, e.g., varying meteoric water influence (Immenhauser et al., 2003), water aging (Patterson and Walter, 1994), increased weathered carbonate input (Melchin and Holmden, 2006), or varying photosynthetic activity (LaPorte et al., 2009). But most importantly, correlation of these offset excursions has been demonstrated in sections with tight biostratigraphic constraints, such as the Aptian (Di Lucia et al., 2012), Cenomanian (Jarvis et al., 2006), Carboniferous (Immenhauser et al., 2003), Silurian (Cramer et al., 2010), and Ordovician (LaPorte et al., 2009). Furthermore, these $\delta^{13}C_{carb}$ excursions and offsets appear unaffected by changing lithology.

There are diagenetic processes known to alter $\delta^{13}C_{carb}$ from the original seawater values. These include meteoric diagenesis, burial diagenesis, aragonite versus calcite precipitation, and the oxidation or production of organic matter (Algeo et al., 1992; Immenhauser et al., 2002; Swart et al., 2009; Colombie et al., 2011). However, none of these appears to explain the positive $\delta^{13}C_{carb}$ excursion of the *extraordinarius* zone.

Early meteoric diagenesis is related to sea level drop and the exposure of sediments to freshwater and sometimes soil zone CO_2 (Allan and Matthews, 1982; Immenhauser et al., 2002). This causes a negative shift in both $\delta^{13}C_{carb}$ and $\delta^{18}O_{carb}$. As such, a correlation between $\delta^{18}O_{carb}$ and $\delta^{13}C_{carb}$ is traditionally viewed as an indicator of meteoric diagenesis (Banner and Hanson, 1990; Algeo et al., 1992) (Fig. 4A for the data from this study). Since meteoric diagenesis drives $\delta^{13}C_{carb}$ to more negative values, the positive *extraordinarius* $\delta^{13}C_{carb}$ excursion cannot be explained by this process. However, the negative $\delta^{13}C_{carb}$ excursion ($\delta^{13}C_{carb}$ almost −8‰) is seen at the peak of the second, more intense, glacial pulse in the Kuanyinchiao Formation (Fig. 2). This coincidence of glacioeustatic shallowing and very negative $\delta^{13}C_{carb}$ values suggests early meteoric diagenesis (Immenhauser et al., 2002). However, $\delta^{18}O_{carb}$ shows no negative excursion. Two explanations are possible. Firstly, the $\delta^{13}C_{carb}$ signal was preserved while the depleted $\delta^{18}O_{carb}$ values were reset through deep burial diagenesis, wherein oxygen in pore waters re-equilibrated with carbonate oxygen under heat and pressure (Algeo et al., 1992; Immenhauser et al., 2002). Alternatively, this negative $\delta^{13}C_{carb}$ spike reflects the primary global seawater signal, which is also seen in the *persculptus* zone of the Blackstone Range (Yukon) (Fig. 3) but is not identified in other sections because of insufficient sampling detail. Detailed sampling of geographically widespread sections would be required to confirm this.

Another diagenetic possibility is that arising from local organic matter oxidation, providing ^{13}C-depleted carbonate, which could alter $\delta^{13}C_{carb}$ within the sediment (Joachimski, 1994). Evidence for this possibility is seen by plotting %TOC against $\delta^{13}C_{carb}$. For the sediments where there is significant carbonate (>10%) there is no correlation (Fig. 4B). However, a weak correlation ($R^2 = 0.28$) is exhibited in sediments where carbonate content is under 10% (*pacificus*, upper *persculptus* and lower *ascensus* zones). This result is expected as a high carbonate content would buffer against any contamination from organic matter. Also, this result does not affect the integrity of the positive $\delta^{13}C_{carb}$ excursion as it occurs within the sediments where carbonate content is >10%. The smooth profile of the $\delta^{13}C_{carb}$ curve in the *extraordinarius* zone, despite changes in %TOC and carbonate content, suggests

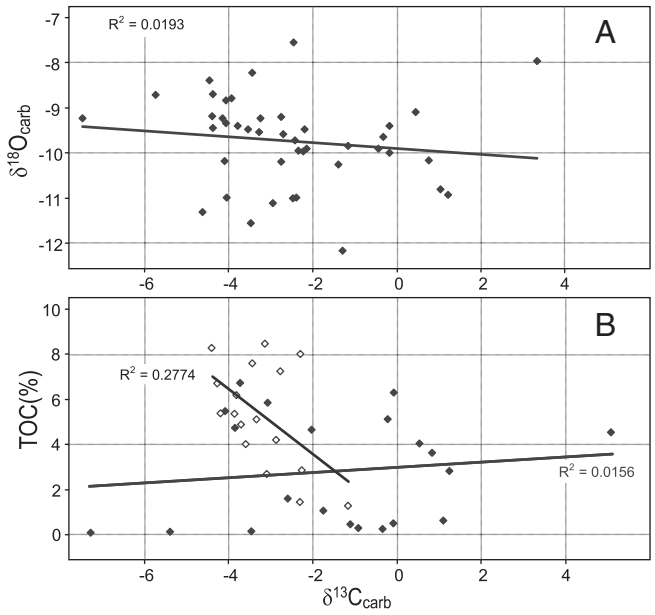

Fig. 4. A. Crossplot of $\delta^{13}C_{carb}$ versus $\delta^{18}O_{carb}$, showing regression line, correlation coefficient (R^2). Note poor correlation. B. Crossplot of $\delta^{13}C_{carb}$ versus %TOC. White points are from samples with <10% carbonate content, black points are from samples with >10% carbonate content. Regression lines and correlation coefficients (R^2) shown for both data sets.

the cause of the excursion was $\delta^{13}C$ changes in the overlying water and that the data were not significantly altered during diagenesis.

Another source of $\delta^{13}C_{carb}$ variation arises from differences in mineralogy. Laboratory experiments have shown that aragonite is enriched in ^{13}C by about 1.7‰ compared to calcite precipitated from the same water (Romanek et al., 1992). Observations from natural environments have shown an even greater difference, up to 4–5‰ (e.g., Swart, 2008). As aragonite is not easily preserved in the sedimentary record, it is not easy to determine what role variable mineralogy had in the Wangjiawan (Riverside) $\delta^{13}C_{carb}$ values. However, as the Hirnantian $\delta^{13}C_{carb}$ excursion is global, and recognized in sections from varying water depths and lithologies, it cannot be attributed to local aragonite formation. Alternatively, it is possible that an increase in global seawater Mg^{2+} could have led to widespread aragonite formation (de Choudens-Sanchez and Gonzalez, 2009). However, a rapid global Mg^{2+} increase and subsequent decrease within about a million years (the duration of the $\delta^{13}C_{carb}$ excursion) would be unlikely as the residence time of magnesium in the oceans is currently about 13 million years (Broecker and Peng, 1982).

Thus, the positive $\delta^{13}C_{carb}$ excursion in the *extraordinarius* zone is most probably a reliable chemostratigraphic tool. It is unlikely that diagenetic factors created a positive excursion, where there was not one, and that such an excursion would be of the same timing and magnitude as is recorded in other sections worldwide. However, the negative spike in the Kuanyinchiao Formation is probably the result of diagenetic influences. Also, where the carbonate content is less than 10%, there may be some diagenetic alteration due to organic matter oxidation, but this does not include the positive or negative $\delta^{13}C_{carb}$ excursions.

5.3. $\delta^{13}C_{org}$, $\delta^{13}C_{carb}$ and stratigraphic correlations

The Wangjiawan data show that the $\delta^{13}C_{carb}$ excursion begins at the base of, or just below, the *extraordinarius* zone (see Fig. 2) and peaks within the *extraordinarius* zone. The $\delta^{13}C_{org}$ curve also begins to rise in parallel with the $\delta^{13}C_{carb}$, but peaks in the Hirnantian Fauna zone, coincident with a negative spike in $\delta^{13}C_{carb}$ values. As Chen et al. (2005b, 2006) have identified the upper half of the Kuanyinchiao Formation to be the basal *persculptus* graptolite zone, it places the $\delta^{13}C_{org}$ peak in the lower *persculptus* zone. Thus, the $\delta^{13}C_{carb}$ and $\delta^{13}C_{org}$ data reach their peak values in different biozones.

This pattern of $\delta^{13}C_{carb}$ and $\delta^{13}C_{org}$ starting to rise near the *pacificus–extraordinarius* boundary is evident in other sections where graptolite stratigraphy is available (Fig. 3). $\delta^{13}C_{carb}$ also peaks in the *extraordinarius* zone (Fig. 3), with the exception of the Vinini Creek section, Nevada (Fig. 3; LaPorte et al., 2009). $\delta^{13}C_{org}$ is not as consistent, peaking in either the *extraordinarius* (e.g., Monitor Range, Nevada; LaPorte et al., 2009) or the *persculptus* (e.g., Dob's Linn, Scotland; Underwood et al., 1997) zones, or plateauing throughout (e.g., Vinini Creek, Nevada; LaPorte et al., 2009). But $\delta^{13}C_{carb}$ and $\delta^{13}C_{org}$ all return to baseline values in the *persculptus* zone (Fig. 3), marking the end of the Hirnantian carbon-isotope excursion. The rise in $\delta^{13}C_{carb}$ and $\delta^{13}C_{org}$ in the late *pacificus*–early *extraordinarius* zones and the return to baseline values in the *persculptus* zone appear to be the most significant chemostratigraphic features.

At Anticosti Island and Estonia, where graptolite stratigraphy is poorly constrained (Delabroye and Vecoli, 2010), chitinozoans are used (Fig. 3). However, debate arises in the correlation of chitinozoan with graptolite biozones. Some workers (e.g., Melchin and Holmden, 2006; Fan et al., 2009; Achab et al., 2011) correlate the chitinozoans *taugourdeaui* and *scabra* with the graptolite *persculptus* zone. However, Baltic stratigraphers (e.g., Brenchley et al., 2003; Kaljo et al., 2007, 2008) place *taugourdeaui* and *scabra* within the *extraordinarius* zone (see Delabroye and Vecoli (2010) and Young et al. (2010) for reviews of the biostratigraphic debate).

Workers preferring the former correlation scheme (*taugourdeaui* + *scabra* = *persculptus*) have based this on the correlation of Anticosti/Estonian $\delta^{13}C_{carb}$ profiles with the $\delta^{13}C_{org}$ profiles of Wangjiawan and Dob's Linn (e.g., Achab et al., 2011). This scheme matches the shallow rises in the *extraordinarius* zone and strong rises in the *persculptus* zone. However, comparison of the Anticosti/Estonian $\delta^{13}C_{carb}$ curves with other profiles shows that the *taugourdeaui* + *scabra* = *persculptus* scheme is ill fitting (see dashed lines in Fig. 3). All $\delta^{13}C_{carb}$ curves show the strongest rise near the *pacificus–extraordinarius* zone. Furthermore, in the graptolite-zoned sections once the Hirnantian carbon-isotope excursion begins, both $\delta^{13}C_{carb}$ and $\delta^{13}C_{org}$ values remain elevated until returning to baseline in the *persculptus* zone (Jones et al., 2011). This condition is broken in the Anticosti $\delta^{13}C_{carb}$ profile if the *taugourdeaui* + *scabra* = *persculptus* scheme is adopted (Fig. 3).

By correlating the *taugourdeaui* and *scabra* chitinozoan zones with the *extraordinarius* zone, the Anticosti/Estonian $\delta^{13}C_{carb}$ and $\delta^{13}C_{org}$ curves produce a much more comfortable fit with the graptolite-zoned sections, and conform to the pattern of beginning in the *extraordinarius* zone and ending in the *persculptus* zone (Fig. 3).

Thus, the Baltic stratigraphers appear correct in correlating the *taugourdeaui* and *scabra* chitinozoan zones with the *extraordinarius* zone. This scheme would also predict that a $\delta^{13}C_{carb}$ analysis of the Dob's Linn section, Scotland, the GSSP for the base of the Silurian – if at all possible – would also show a $\delta^{13}C_{carb}$ excursion beginning in the near the *pacificus–extraordinarius* zone even though it shows a $\delta^{13}C_{org}$ peak in the *persculptus* zone.

The Wangjiawan (Riverside) carbon isotope data also cautions against assuming that the $\delta^{13}C_{org}$ profile will necessarily match the $\delta^{13}C_{carb}$ profile. $\delta^{13}C_{carb}$ values are derived from local seawater dissolved inorganic carbonate $\delta^{13}C_{DIC}$ and can be diagenetically altered (as outlined in Section 5.2). $\delta^{13}C_{org}$ values are the result of photosynthetic activity taking carbon from atmospheric and dissolved CO_2, indicating some connection between $\delta^{13}C_{org}$ and $\delta^{13}C_{carb}$. However, different primary producers can fractionate carbon differently (e.g., Pancost et al., 1999; Takahashi et al., 2010). Also, varying environmental conditions can alter the rate of carbon fixation that, in turn, can alter $\delta^{13}C_{org}$ (Laws et al., 1995). Furthermore, the degree of remineralization can also affect $\delta^{13}C_{org}$ (Burdige, 2007). Given that the $\delta^{13}C_{org}$ peak occurs in the Kuanyinchiao Formation where TOC is diminished, it may indicate that a different primary producer was more prominent. This may

also tie in with the sulfur isotope results, where it is possible that the elevated $\delta^{34}S_{sulfide}$ of the Kuanyinchiao Formation was the result of a more reactive organic matter supply that increased sulfate reduction rates (Section 5.1).

The consistent pattern of $\delta^{13}C_{org}$ profiles across the Yangtze Platform at Wangjiawan (Wang et al., 1997; Fan et al., 2009), Huanghuachang (Wang et al., 1997), Nanbazi (Yan et al., 2009), and Fenxiang (Wang et al., 1997) indicates that whatever factors caused the $\delta^{13}C_{org}$ shifts, these have to be basin-wide mechanisms.

5.4. $\delta^{13}C$ rise and Hirnantian environmental events

Explanations for the Hirnantian $\delta^{13}C$ excursion have fallen into two camps. According to the first, the rise of $\delta^{13}C$ is attributed to an increase in primary productivity and organic burial which sequesters ^{12}C, leaving the inorganic carbon pool enriched in ^{13}C (e.g., Marshall and Middleton, 1990; Brenchley et al., 1994; Marshall et al., 1997; Brenchley et al., 2003). This is known as the "productivity" hypothesis. On the other hand, the second explanation invokes an alteration of weathering patterns due to ice sheets covering high-latitude land, but lowered sea levels exposing more carbonate platforms in lower latitudes (e.g., Kump et al., 1999; Melchin and Holmden, 2006). This is known as the "weathering" hypothesis. Workers suggest that carbonate platforms were preferentially exposed during the glacial sea level fall, providing more carbonate and less organic matter for weathering. Silicate weathering was also reduced as ice sheets covered continental Gondwana, leading to a build up of CO_2 in the atmosphere (Kump et al., 1999) until sufficient greenhouse warming caused the deglaciation.

The available TOC data (Fig. 3) argues against the productivity hypothesis. If increased organic matter burial was responsible for the positive $\delta^{13}C_{carb}$ and $\delta^{13}C_{org}$ excursions, then a coincident increase in TOC would be expected. But TOC actually declines in most sections coincident with the elevated $\delta^{13}C$ values. Although one could argue for organic matter deposition in some yet to be analyzed basin, or even the deep sea, the available evidence is not favorable to this hypothesis. Other sections, not shown in Fig. 3, that also show low TOC at this interval include Nanbazi (China; Yan et al., 2009), Cape Manning and Truro Lake (Arctic Canada; Melchin and Holmden, 2006).

The weathering hypothesis could be bolstered by examples of positive $\delta^{13}C_{carb}$ excursions coincident with sea level falls. Comparable events could be the Carboniferous–Permian glaciations, which occasionally show coincident $\delta^{13}C$ shifts, although they are not as consistent as the Hirnantian (Mii et al., 2001; Grossman et al., 2008; Birgenheier et al., 2010; Buggisch et al., 2011). On the other hand, the Pleistocene glacial cycles show $\delta^{13}C_{carb}$ falling during glacial maxima (i.e., sea level minima) (e.g., Curry and Oppo, 2005), indicating that an increased weathering of carbonate is not significant. However, one could argue that carbonate platforms were much more extensive during the Paleozoic compared with the Pleistocene (Kump et al., 1999).

The lack of consensus on the interpretation of the $\delta^{13}C$ shifts (during the Hirnantian, as well as other time periods) hampers our ability to robustly interpret the events causing this geochemical signal. Understanding the causal relationships between the Hirnantian glaciation and carbon-cycle perturbation may await a more fundamental understanding of the mechanisms behind the $\delta^{13}C$ signal.

6. Conclusions

New geochemical data provide a record of changing environmental conditions associated with the Hirnantian of South China. Two glacial pulses coincide with increases in sediment carbonate content. $\delta^{34}S_{sulfide}$ data shows elevated values in the Kuanyinchiao Formation, consistent with other sections throughout the Yangtze Platform. However, there is no consensus on the cause of these changes.

New $\delta^{13}C_{carb}$ data shows a peak in the *extraordinarius* zone, before the well-established $\delta^{13}C_{org}$ peak in the *persculptus* zone. Previous global Hirnantian correlations have matched $\delta^{13}C_{carb}$ peaks with the Wangjiawan $\delta^{13}C_{org}$ peak, making correlative sections comparatively too young and promoting a correlation of *taugourdeaui* and *scabra* chitinozoans with the *persculptus* graptolite zone. Instead, the new data suggests that the *taugourdeaui* and *scabra* zones correlate with the *extraordinarius* zone. Although the ultimate cause of the Hirnantian glaciation and its relationship to the $\delta^{13}C_{carb}$ perturbation remain elusive, the new data and refined correlation framework presented here provide another step toward addressing these issues.

Acknowledgments

P.G. and D.A.F. were partially supported by a grant from the Agouron Institute. K.K. was partly supported by a grant-in-aid for scientific research from the Ministry of Education, Science and Culture of Japan. Thanks to Dwight McCay for contributions to data generation. Thanks also go to two anonymous reviewers and the editor (F. Surlyk) whose contributions greatly improved the manuscript.

References

Achab, A., Asselin, E., Desrochers, A., Riva, J.F., Farley, C., 2011. Chitinozoan biostratigraphy of a new Upper Ordovician stratigraphic framework for Anticosti Island, Canada. Geological Society of America Bulletin 123, 186–205.
Algeo, T.J., Lohmann, K.C., Wilkinson, B.H., 1992. Meteoric-burial diagenesis of middle Pennsylvanian limestones in the Orogrande Basin, New Mexico: water/rock interactions and basin geothermics. Journal of Sedimentary Petrology 62, 652–670.
Allan, J.R., Matthews, R.K., 1982. Isotope signatures associated with early meteoric diagenesis. Sedimentology 29, 797–817.
Bambach, R.K., Knoll, A.H., Wang, S.C., 2004. Origination, extinction, and mass depletions of marine diversity. Paleobiology 30, 522–542.
Banner, J.L., Hanson, G.H., 1990. Calculation of simultaneous isotopic and trace element variations during water-rock interaction with application to carbonate diagenesis. Geochimica et Cosmochimica Acta 54, 3123–3137.
Berner, R.A., 1978. Sulfate reduction and the rate of deposition of marine sediments. Earth and Planetary Science Letters 37, 492–498.
Berner, R.A., 1984. Sedimentary pyrite formation: An update. Geochimica et Cosmochimica Acta 48, 605–615.
Birgenheier, L.P., Frank, T.D., Fielding, C.R., Rygel, M.C., 2010. Coupled carbon isotopic and sedimentological records from the Permian system of eastern Australia reveal the response of atmospheric carbon dioxide to glacial growth and decay during the late Palaeozoic Ice Age. Palaeogeography, Palaeoclimatology, Palaeoecology 286, 178–193.
Brenchley, P.J., Marshall, J.D., Carden, G.A.F., Robertson, D.B.R., Long, D.G.F., Meidla, T., Hints, L., Anderson, T.F., 1994. Bathymetric and isotopic evidence for a short–lived Late Ordovician glaciation in a greenhouse period. Geology 22, 295–298.
Brenchley, P.J., Carden, G.A.F., Hints, L., Kaljo, D., Marshall, J.D., Martma, T., Meidla, T., Nolvak, J., 2003. High-resolution stable isotope stratigraphy of Upper Ordovician sequences: constraints on the timing of bioevents and environmental changes associated with mass extinction and glaciation. Geological Society of America Bulletin 115, 89–104.
Broecker, W.S., Peng, T.-H., 1982. Tracers in the Sea. Eldigo Press, NY Palisades.
Buggisch, W., Wang, X., Alekseev, A.S., Joachimski, M.M., 2011. Carboniferous–Permian carbon isotope stratigraphy of successions from China (Yangtze platform), USA (Kansas) and Russia (Moscow Basin and Urals). Palaeogeography, Palaeoclimatology, Palaeoecology 301, 18–38.
Burdige, D.J., 2007. The preservation of organic matter in marine sediments: controls, mechanisms and an imbalance in sediment organic carbon budgets? Chemical Reviews 107, 467–485.
Burton, E.D., Sullivan, L.A., Bush, R.T., Johnston, S.G., Keene, A.F., 2008. A simple and inexpensive chromium-reducible sulfur method for acid-sulfate soils. Applied Geochemistry 23, 2759–2766.
Canfield, D.E., 2001. Geochemistry of sulphur isotopes. In: Valley, J.W., Cole, D.R. (Eds.), Stable Isotope Geochemistry: Mineralogical Society of America Reviews and Mineralogy and Geochemistry, vol. 43, pp. 607–636. Washington D.C.
Canfield, D.E., Raiswell, R., Westrich, J.T., Reaves, C.M., Berner, R.A., 1986. Chemical Geology 54, 149–155.
Chambers, L.A., 1982. Sulfur isotope study of a modern intertidal environment, and the interpretation of ancient sulfides. Geochimica et Cosmochimica Acta 46, 721–728.
Chen, X., Rong, J., Mitchell, C.E., Harper, D.A.T., Fan, J.-X., Zhan, R., Zhang, Y., Li, R., Wang, Y., 2000. Late Ordovician to earliest Silurian graptolite and brachiopod biozonation from the Yangtze region, South China, with a global correlation. Geological Magazine 137, 623–650.
Chen, X., Rong, J.Y., Li, Y., Boucott, A.J., 2004. Facies patterns and geography of the Yangtze region, South China, through the Ordovician and Silurian transition. Palaeogeography, Palaeoclimatology, Palaeoecology 204, 353–372.
Chen, X., Fan, J.-X., Melchin, M.J., Mitchell, C.E., 2005a. Hirnantian (latest Ordovician) graptolites from the Upper Yangtze region, China. Palaeontology 48, 235–280.
Chen, X., Melchin, M.J., Sheets, H.D., 2005b. Patterns and processes of latest Ordovician graptolite extinction and recovery based on data from south China. Journal of Paleontology 79, 842–861.

Chen, X., Rong, J.-Y., Fan, J.-X., Zhan, R.-B., Mitchell, C.E., Harper, D.A.T., Melchin, M.J., Peng, P.A., Finney, S.C., Wang, X.-F., 2006. The Global Stratotype Section and Point (GSSP) for the base of the Hirnantian Stage (the uppermost of the Ordovician System). Episodes 29, 183–196.

Colombie, C., Lecuyer, C., Strasser, A., 2011. Carbon- and oxygen-isotope records of palaeoenvironmental and carbonate production changes in shallow-marine carbonates (Kimmeridgian, Swiss Jura). Geological Magazine 148, 133–153.

Copper, P., 2001. Reefs during the multiple crises towards the Ordovician–Silurian boundary: Anticosti Island, eastern Canada, and worldwide. Canadian Journal of Earth Sciences 38, 153–171.

Cramer, B.D., Loydell, D.K., Samtleben, C., Munnecke, A., Kaljo, D., Männik, P., Martma, T., Jeppsson, L., Kleffner, M.A., Barrick, J.E., Johnson, C.A., Emsbo, P., Joachimski, M.M., Bickert, T., Saltzman, M.R., 2010. Testing the limits of Paleozoic chronostratigraphic correlation via high-resolution (<500 k.y.) integrated conodont, graptolite, and carbon isotope ($\delta^{13}C_{carb}$) biochemostratigraphy across the Llandovery–Wenlock (Silurian) boundary: is a unified Phanerozoic time scale achievable? Geological Society of America Bulletin 122, 1700–1716.

Curry, W.B., Oppo, D.W., 2005. Glacial water mass geometry and the distribution of $\delta^{13}C$ of ΣCO_2 in the western Atlantic Ocean. Palaeoceanography 20, PA1017.

De Choudens-Sanchez, V., Gonzalez, L.A., 2009. Calcite and aragonite precipitation under controlled instantaneous supersaturation: elucidating the role of $CaCO_3$ saturation state and Mg/Ca ratio on calcium carbonate polymorphism. Journal of Sedimentary Research 79, 363–376.

Delabroye, A., Vecoli, M., 2010. The end-Ordovician glaciation and the Hirnantian Stage: a global review and questions about the Late Ordovician event stratigraphy. Earth-Science Reviews 98, 269–282.

Deynoux, M., 1985. Terrestrial or waterlain glacial diamictites? Three case studies from the Late Precambrian and Late Ordovician glacial drifts in West Africa. Palaeogeography, Palaeoclimatology, Palaeoecology 51, 97–141.

Deynoux, M., Trompette, R., 1981. Late Ordovician tillites of the Taoudeni Basin, West Africa. In: Hambrey, M.J., Harland, W.B. (Eds.), Earth's Pre-Pleistocene Glacial Record. Cambridge University Press, Cambridge, pp. 89–96.

Di Lucia, M., Trecalli, A., Mutti, M., Parente, M., 2012. Bio-chemostratigraphy of the Barremian–Aptian shallow-water carbonates of the southern Apennines (Italy): pinpointing the OAE1a in a Tethyan carbonate platform. Solid Earth 3, 1–28.

Fan, J., Peng, P., Melchin, M.J., 2009. Carbon isotopes and event stratigraphy near the Ordovician–Silurian boundary, Yichang, South China. Palaeogeography, Palaeoclimatology, Palaeoecology 276, 160–169.

Finnegan, S., Bergmann, K., Eiler, J.M., Jones, D.S., Fike, D.A., Eisenman, I., Hughes, N.C., Tripati, A.K., Fischer, W.W., 2011. Magnitude and duration of Late Ordovician–Early Silurian glaciation. Science 331, 903–906.

Finney, S.C., Berry, W.B.N., Cooper, J.D., Ripperdan, R.L., Sweet, W.C., Jacobson, S.R., Soufiane, A., Achab, A., Noble, P.J., 1999. Late Ordovician mass extinction: a new perspective from stratigraphic sections in central Nevada. Geology 27, 215–218.

Ghienne, J.-F., 2003. Late Ordovician sedimentary environments, glacial cycles, and postglacial transgression in the Taoudeni Basin, West Africa. Palaeogeography, Palaeoclimatology, Palaeoecology 189, 117–145.

Ghienne, J.-F., Le Heron, D., Moreau, J., Denis, M., Deynoux, M., 2007. The Late Ordovician glacial sedimentary system of the North Gondwana platform. In: Hambrey, M., Christoffersen, P., Glasser, N., Janssen, P., Hubbard, B., Siegert, M. (Eds.), Glacial Sedimentary Processes and Products. Special Publication. International Association of Sedimentologists, Blackwells, Oxford, pp. 295–319.

Goldhaber, M.B., Kaplan, I.R., 1974. The sulfur cycle. In: Goldberg, E.D. (Ed.), The Sea, Volume 5. Wiley, New York, pp. 569–655.

Gradstein, F.M., Ogg, J.G., Smith, A.G., 2004. A Geologic Time Scale 2004. Cambridge University Press, Cambridge, UK.

Grossman, E.L., Yancey, T.E., Jones, T.E., Bruckschen, P., Chuvashov, B., Mazzullo, S.J., Mii, H.-S., 2008. Glaciation, aridification, and carbon sequestration in the Permo-Carboniferous: the isotopic record from low latitudes. Palaeogeography, Palaeoclimatology, Palaeoecology 268, 222–233.

Habicht, K.S., Canfield, D.E., 1997. Sulfur isotope fractionation during bacterial sulfate reduction in organic-rich sediments. Geochimica et Cosmochimica Acta 61, 5351–5361.

Habicht, K.S., Canfield, D.E., 2001. Isotope fractionation by sulfate-reducing natural populations and the isotopic composition of sulfide in marine sediments. Geology 29, 555–558.

Immenhauser, A., Kenter, J.A.M., Ganssen, G., Bahamonde, J.R., Van Vliet, A., Saher, M.H., 2002. Origin and significance of isotope shifts in Pennsylvanian carbonates (Asturias, NW Spain). Journal of Sedimentary Research 72, 82–94.

Immenhauser, A., Della Porta, G., Kenter, J.A.M., Bahamonde, J.R., 2003. An alternative model for the positive shifts in shallow-marine carbonate $\delta^{13}C$ and $\delta^{18}O$. Sedimentology 50, 953–959.

Jarvis, I., Gale, A.S., Jenkyns, H.C., Pearce, M.A., 2006. Secular variation in Late Cretaceous carbon isotopes: a new $\delta^{13}C$ carbonate reference curve for the Cenomanian–Campanian (99.6–70.6 Ma). Geological Magazine 143, 561–608.

Joachimski, M.M., 1994. Subaerial exposure and deposition of shallowing-upward sequences: evidence from stable isotopes of Purbeckian peritidal carbonates (basal Cretaceous), Swiss and French Jura Mountains. Sedimentology 41, 805–824.

Jones, D.S., Fike, D.A., Finnegan, S., Fischer, W.W., Schrag, D.P., McCay, D., 2011. Terminal Ordovician carbon isotope stratigraphy and glacioeustatic sea-level change across Anticosti Island (Québec, Canada). Geological Society of America Bulletin 123, 1645–1664.

Kaljo, D., Martma, T., Saadre, T., 2007. Post-Hunnebergian Ordovician carbon isotope trend in Baltoscandia, its environmental implications and some similarities with that of Nevada. Palaeogeography, Palaeoclimatology, Palaeoecology 245, 138–155.

Kaljo, D., Hints, L., Männik, P., Nolvak, J., 2008. The succession of Hirnantian events based on data from Baltica: brachiopods, chitinozoans, conodonts, and carbon isotopes. Estonian Journal of Earth Sciences 57, 197–218.

Kaljo, D., Hints, L., Hints, O., Mannik, P., Martma, T., Nolvak, J., 2011. Katian prelude to the Hirnantian (Late Ordovician) mass extinction: a Baltic perspective. Geological Journal 46, 464–477.

Kump, L.R., Arthur, M.A., Patzkowsky, M.E., Gibbs, M.T., Pinkus, D.S., Sheehan, P.M., 1999. A weathering hypothesis for glaciation at high atmospheric pCO_2 during the Late Ordovician. Palaeogeography, Palaeoclimatology, Palaeoecology 152, 173–187.

LaPorte, D.F., Holmden, C., Patterson, W.P., Loxton, J.D., Melchin, M.J., Mitchell, C.E., Finney, S.C., Sheets, H.D., 2009. Local and global perspectives on carbon and nitrogen cycling during the Hirnantian Glaciation. Palaeogeography, Palaeoclimatology, Palaeoecology 276, 182–195.

Laws, E.A., Popp, B.N., Bidigare, R.R., Kennicutt, M.C., Macko, S.A., 1995. Dependence of phytoplankton carbon isotopic composition on growth rate and $[CO_2]_{aq}$: theoretical considerations and experimental results. Geochimica et Cosmochimica Acta 59, 1131–1138.

Le Heron, D.P., Ghienne, J.-F., El Houicha, M., Khoukhi, K., Rubino, J.-L., 2007. Maximum extent of ice sheets in Morocco during the Late Ordovician glaciation. Palaeogeography, Palaeoclimatology, Palaeoecology 245, 200–226.

Marshall, J.D., Middleton, P.D., 1990. Changes in marine isotopic composition and the Late Ordovician glaciation. Journal of the Geological Society of London 147, 1–4.

Marshall, J.D., Brenchley, P.J., Mason, P., Wolff, G.A., Astini, R.A., Hints, L., Meidla, T., 1997. Global carbon isotopic events associated with mass extinction and glaciation in the late Ordovician. Palaeogeography, Palaeoclimatology, Palaeoecology 132, 195–210.

Melchin, M.J., 2008. Restudy of some Ordovician–Silurian boundary graptolites from Anticosti Island, Canada, and their biostratigraphic significance. Lethaia 41, 155–162.

Melchin, M.J., Holmden, C., 2006. Carbon isotope chemostratigraphy in Arctic Canada: sea-level forcing of carbonate platform weathering and implications for Hirnantian global correlation. Palaeogeography, Palaeoclimatology, Palaeoecology 234, 186–200.

Melchin, M.J., Holmden, C., Williams, S.H., 2003. Correlation of graptolite biozones, chitinozoan biozones, and carbon isotope curves through the Hirnantian. In: Albanesi, G.L., Beresi, M.S., Peralta, S.H. (Eds.), Ordovician from the Andes, INSUEGO, Serie de Correlacion Geologica, vol. 17, pp. 101–104.

Mii, H.-S., Grossman, E.L., Yancey, T.E., Chuvashov, B., Egorov, A., 2001. Isotope records of brachiopod shells from the Russian Platform — evidence for the onset of Mid-Carboniferous glaciation. Chemical Geology 175, 133–147.

Ogg, J.G., Ogg, G., Gradstein, F.M., 2008. A Concise Geologic Time Scale. Cambridge University Press, Cambridge, UK.

Panchuk, K.M., Holmden, C., Kump, L.R., 2005. Sensitivity of the epeiric sea carbon isotope record to local-scale carbon cycle processes: tales from the Mohawkian Sea. Palaeogeography, Palaeoclimatology, Palaeoecology 228, 320–337.

Panchuk, K.M., Holmden, C., Leslie, S.A., 2006. Local controls on carbon cycling in the Ordovician mid-continent region of North America with implications for carbon isotope secular curves. Journal of Sedimentary Research 76, 200–211.

Pancost, R.D., Freeman, K.H., Patzkowsky, M.E., 1999. Organic-matter source variation and the expression of a late Middle Ordovician carbon isotope excursion. Geology 27, 1015–1018.

Patterson, W., Walter, L., 1994. Depletion of ^{13}C in seawater CO_2 on modern carbonate platforms: significance for the carbon isotopic record of carbonates. Geology 22, 885–888.

Riva, J., 1988. Graptolites at and below the Ordovician–Silurian boundary on Anticosti Island, Canada. Bulletin of the British Museum, Natural History. Geology Series, 43, pp. 221–237.

Romanek, C.S., Grossman, E.L., Morse, J.W., 1992. Carbon isotopic fractionation in synthetic aragonite and calcite: effects of temperature and precipitation rate. Geochimica et Cosmochimica Acta 56, 419–430.

Rong, J.-Y., Chen, X., Harper, D.A.T., 2002. The latest Ordovician Hirnantian Fauna (Brachiopoda) in time and space. Lethaia 35, 213–249.

Sheehan, P.M., 2001. The Late Ordovician mass extinction. Annual Review of Earth and Planetary Sciences 29, 331–364.

Sim, M.S., Bosak, T., Ono, S., 2011a. Large sulfur isotope fractionation does not require disproportionation. Science 333, 74–77.

Sim, M.S., Ono, S., Donovan, K., Templer, S.P., Bosak, T., 2011b. Effect of electron donors on the fractionation of sulfur isotopes by a marine *Desulfovibrio* sp. Geochimica et Cosmochimica Acta 75, 4244–4259.

Soufiane, A., Achab, A., 2000. Upper Ordovician and Lower Silurian chitinozoans from central Nevada and Arctic Canada. Review of Palaeobotany and Palynology 113, 165–187.

Swart, P.K., 2008. Global synchronous changes in the carbon isotopic composition of carbonate sediments unrelated to changes in the global carbon cycle. Proceedings of the National Academy of Science 105, 13741–13745.

Swart, P.K., Reijmer, J.J.G., Otto, R., 2009. A re-evaluation of facies on Great Bahama Bank II: variations in the $\delta^{13}C$, $\delta^{18}O$ and mineralogy of surface sediments. In: Swart, P.K., et al. (Ed.), Perspectives in Carbonate Geology: International Association of Sedimentologists Special Publication, 41, pp. 47–59.

Takahashi, S., Kaiho, K., Oba, M., Kakegawa, T., 2010. A smooth negative shift of organic carbon isotope ratios at an end-Permian mass extinction horizon in central pelagic Panthalassa. Palaeogeography, Palaeoclimatology, Palaeoecology 292, 532–539.

Trotter, J.A., Williams, I.A., Barnes, C.R., Lécuyer, C., Nicoll, R.S., 2008. Did cooling oceans trigger Ordovician biodiversification? Evidence from conodont thermometry. Science 321, 550–554.

Underwood, C.J., Crowley, S.F., Marshall, J.D., Brenchley, P.J., 1997. High-resolution carbon isotope stratigraphy of the basal Silurian Stratotype (Dob's Linn, Scotland) and its global correlation. Journal of the Geological Society of London 154, 709–718.

Vandenbroucke, T.R.A., Chen, X., Verniers, J., 2005. A study on the preliminary results of latest Ordovician chitinozoan from Wangjiawan, Yichang, China. Acta Palaeontologica Sinica 44, 203–208.

Wang, K., Chatterton, B.D.E., Wang, Y., 1997. An organic carbon isotope record of Late Ordovician to Early Silurian marine sedimentary rocks, Yangtze Sea, South China:

implications for CO_2 changes during the Hirnantian glaciation. Palaeogeography, Palaeoclimatology, Palaeoecology 132, 147–158.
Yan, D., Chen, D., Wang, Q., Wang, J., Chu, Y., 2008. Environmental redox changes of the Yangtze Sea during the Ordo-Silurian transition. Acta Geologica Sinica (English Edition) 82, 679–689.
Yan, D.T., Chen, D.Z., Wang, Q.C., Wang, J.G., Wang, Z.Z., 2009. Carbon and sulfur isotopic anomalies across the Ordovician–Silurian boundary on the Yangtze Platform, South China. Palaeogeography, Palaeoclimatology, Palaeoecology 274, 32–39.
Yan, D., Chen, D., Wang, Q., Wang, J., 2010. Large-scale climatic fluctuations in the latest Ordovician on the Yangtze block, south China. Geology 38, 599–602.
Young, S.A., Saltzman, M.R., Ausich, W.I., Desrochers, A., Kaljo, D., 2010. Did changes in atmospheric CO_2 coincide with latest Ordovician glacial interglacial cycles? Palaeogeography, Palaeoclimatology, Palaeoecology 296, 376–388.
Zhang, T., Kershaw, S., Wan, Y., Lan, G., 2000. Geochemical and facies evidence for palaeoenvironmental change during the Late Ordovician Hirnantian glaciation in South Sichuan Province, China. Global and Planetary Change 24, 133–152.
Zhang, T., Shen, Y., Zhan, R., Shen, S., Chen, X., 2009. Large perturbations of the carbon and sulfur cycle associated with the Late Ordovician mass extinction in South China. Geology 37, 299–302.